Dynamic Enolate Recognition in Aqueous Solution by Zinc(II) in a Phenacyl-Pendant Cyclen Complex: Implications for the Role of Zinc(II) in Class II Aldolases

Eiichi Kimura,*,† Teruhiro Gotoh,† Tohru Koike,† and Motoo Shiro‡

Contribution from the Department of Medicinal Chemistry, Faculty of Medicine, Hiroshima University, Kasumi 1-2-3, Minami-ku, Hiroshima 734-8551, Japan, and Rigaku Corporation X-ray Research Laboratory, Matsubaracho 3-9-12, Akishima, Tokyo 196-8666, Japan

Received August 12, 1998

Abstract: A zinc(II) complex of 1-(4-bromophenacyl)-1,4,7,10-tetraazacyclododecane, ZnL, has been synthesized to mimic the active center of class II aldolases. Its X-ray crystal structure showed that zinc(II) remains atop the four nitrogen atoms of cyclen (average Zn−N distance 2.170 Å) to bind with the carbonyl oxygen (Zn−O distance of 2.159(3) Å) and one H_2O (Zn−O distance of 2.130(3) Å). Crystal data: monoclinic, space group $P2_1/n$ (No. 14), with $a = 12.221(8)$ Å, $b = 11.052(7)$ Å, $c = 18.194(9)$ Å, $\beta = 97.12(3)°$, $V = 2438(5)$ Å^3, $Z = 4$, $R = 0.041$, and $R_w = 0.046$. The potentiometric pH titration of ZnL in aqueous solution disclosed dissociation of one proton with $pK_a = 8.41$ at 25 °C and $I = 0.1$ ($NaClO_4$), which yields a mixture of a hydroxide-bound complex (ZnL−OH^-) and an enolate-bound complex ($ZnH_{-1}L$) in a 3:1 ratio, as determined by UV spectrophotometric and ^{13}C and ^1H NMR titrations. This is the first quantitative assessment of enolate formation promoted by a proximate zinc(II) ion near neutral pH in aqueous solution. The enolate-bound complex $ZnH_{-1}L$ independently isolated by treatment of ZnL with an equivalent amount NaOMe in acetonitrile was fully characterized to compare with ZnL. The equilibrium between the ZnL−OH^- and $ZnH_{-1}L$ varied with temperature (15, 25, and 35 °C), from which thermodynamic parameters of $\Delta G = 3.0$ kJ mol^{-1}, $\Delta H = 8.7$ kJ mol^{-1}, and $\Delta S = 19$ J mol^{-1} K^{-1} at 25 °C were determined. Because of the facile enolization by zinc(II), the methylene hydrogen atoms (adjacent to the carbonyl) of ZnL were readily exchanged by deuterium under physiological conditions. The half-life at 25 °C for this H−D exchange at pD 7 (20 mM MOPS buffer) was determined to be 25 min by ^1H NMR measurements. Implications of the present results for the role of zinc(II) in the active center of class II aldolases are discussed.

Introduction

Aldolases are enzymes catalyzing reversible stereospecific aldol condensation. For example, fructose 1,6-bis(phosphate) aldolase (FBP-aldolase, EC 4.1.2.13) catalyzes the cleavage of D-fructose 1,6-bis(phosphate) (FBP) to dihydroxyacetone phosphate (DHAP) and D-glyceraldehyde 3-phosphate (G3P) and the reverse formation of FBP from DHAP and G3P (see Scheme 1).[1] Aldolases are classified into two groups on the basis of reaction mechanism. Class I aldolases, which occur in animals and plants, form a Schiff base intermediate between the ϵ-amino group of the lysine residue and the carbonyl group of the sugar.[2] Class II aldolases, which occur in yeasts and *Escherichia coli*, use the zinc(II) ion, which acts as a Lewis acid in the active site.[3] In the X-ray structure of the class II fuculose 1-phosphate aldolase (FucA, EC 4.1.2.17) produced by *E. coli*,[4] the zinc(II) ion binds to three imidazole groups of His(92, 94, 115) and one carboxylate of Glu(73). On the basis of the X-ray crystal structure of FucA complexed with phosphoglycolohydroxamate as a substrate analogue or an inhibitor, a role of the zinc(II) ion was proposed to stabilize the enediolate-DHAP intermediate **1** for the aldol condensation.[5] From the ^{13}C NMR study of *E. coli* FBP-aldolase, Szwergold et al. found pH-dependent (the optimum pH 9.0 and higher, 50% maximum pH 8.0) formation of the enediol (or enediolate)-DHAP intermediate from the FBP substrate.[6] All of these observations also suggest the role of

Scheme 1

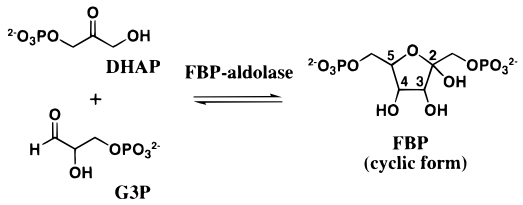

* Corresponding author. E-mail: ekimura@ipc.hiroshima-u.ac.jp.
† Hiroshima University.
‡ Rigaku Corp.

(1) Book reviews: (a) Walsh, C. *Enzymatic Reaction Mechanisms*; Freeman and Co.: New York, 1979. (b) Wong, C.-H.; Whitesides, G. M. *Enzymes in Synthetic Organic Chemistry*; Pergamon Press: Oxford, U.K., 1994. (c) Voet, D.; Voet, J. G. *Biochemistry*; Wiley & Sons: New York, 1990.

(2) (a) Sygusch, J.; Beaudry, D.; Allaire, M. *Proc. Natl. Acad. Sci. U.S.A.* **1987**, 84, 7846−7850. (b) Gamblin, S. J.; Davies, G. J.; Grimes, J. M.; Jackson, R. M.; Littlechild, J. A.; Watson, H. C. *J. Mol. Biol.* **1991**, *219*, 573−576. (c) Hester, G.; Brenner-Holzach, O.; Rossi, F. A.; Struck-Donatz, M.; Winterhalter, K. H.; Smit, J. D. G.; Piontek, K. *FEBS Lett.* **1991**, 237−242.

(3) Kobes, R. D.; Simpson, R. T.; Vallee, B. L.; Rutter, W. J. *Biochemistry* **1969**, *8*, 585−588.

(4) Dreyer, M. K.; Schulz, G. E. *J. Mol. Biol.* **1993**, *231*, 549−553.

(5) (a) Dreyer, M. K.; Schulz, G. E. *J. Mol. Biol.* **1996**, *259*, 458−466. (b) Fessner, W.-D.; Schneider, A.; Held, H.; Sinerius, G.; Walter, C.; Hixon, M.; Schloss, J. V. *Angew. Chem., Int. Ed. Engl.* **1996**, *35*, 2219−2221.

(6) Szwergold, B. S.; Ugurbil, K.; Brown, T. R. *Arch. Biochem. Biophys.* **1995**, *317*, 244−252.

10.1021/ja982904e CCC: $18.00
Published on Web 02/02/1999

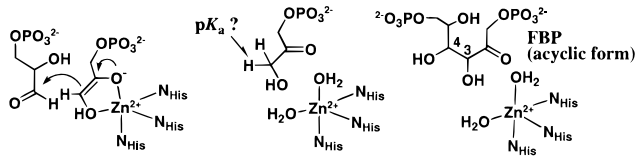

1 **2** **3**

zinc(II) in polarizing the carbonyl bond to increase the acidity of the adjacent hydrogen in **2**, which then is readily abstracted by a weak (general) base, glutamic carboxylate. However, for the reversible mechanism of the aldol reaction, no clear picture is presented. Moreover, in the recent X-ray crystal structure of another class II *E. coli* FBP-aldolase, direct interaction of FBP, DHAP, and G3P with the zinc(II) ion seems difficult, but rather the water molecules bound to the zinc(II) ion are more accessible to those substrates.[7] Chemical elucidation of the reaction mechanism of class II aldolases has remained totally unexplored: the most fundamental chemical question is, How much is the pK_a value of the active methylene lowered by the zinc(II) ion in **2**? Another question is whether the zinc(II) ion is involved in deprotonation of the C4 hydroxyl hydrogen of the acyclic form of FBP in **3** to produce DHAP and G3P.

In organic synthesis, carbonyl activation procedures have been long used for aldol condensation.[8] For acid-catalyzed aldol condensation, strong Lewis acids (such as H^+ and La^{3+}), which are biologically unacceptable, have been used in aqueous solution or in aprotic solvents. For base-catalyzed aldol condensation, extremely strong bases (e.g., $LiNH_2$) have been used in aprotic solvents. The use of these strong acids and bases in aqueous or aprotic solvents may be avoided if we know accurate pK_a values of enolates bound to mild acids such as the zinc(II) ion in aqueous solution. It is of interest to recall a classic metal-assisted aldol condensation (see Scheme 2): Copper(II)−(glycine)$_2$ complex **4** in strong alkaline solution (pH >11) reacts with acetaldehyde to yield the threonine complex **5** ("Akabori reaction").[9]

In our studies of other zinc(II) enzyme models,[10−20] we elucidated the role of Ser(102) and the zinc(II) ion in alkaline

Scheme 2

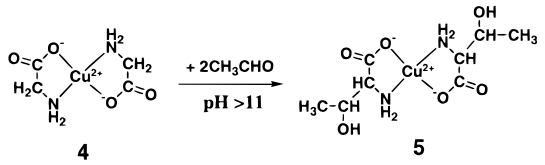

4 **5**

Scheme 3

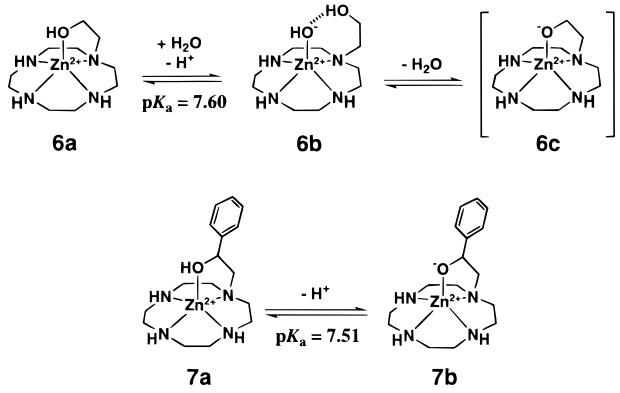

6a **6b** **6c** **7a** **7b**

phosphatase by utilizing zinc(II) complexes of two different alcohol-pendant 1,4,7,10-tetraazacyclododecane (cyclen) compounds, **6** and **7** (see Scheme 3).[17,18] Each zinc(II) ion is coordinated by four nitrogen atoms of cyclen in the proximity of the alcoholic group. The electrostatic effect of the zinc(II) ions indirectly (through **6b**)[17] or directly[18] yielded the alkoxide complexes **6c** and **7b** with pK_a values of 7.60 and 7.51, respectively. Thus the zinc(II) ion served to lower the pK_a values of the alcohols (ca. 15) by 7−8 units, a fact leading to a postulate that the FBP alcohol may be directly or indirectly deprotonated for the reverse aldol condensation in **3**. We also found that the cyclen-attached uracil zinc(II) complex **8** yielded the C(4)-

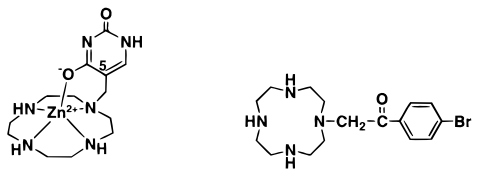

8 **9**

enolate O^- structure with pK_a = 6.0.[21] Therefore, the zinc(II) ion in cyclen will serve an excellent probe to study the detailed acidic role of zinc(II) in the aldol condensation. We thus have designed 1-(4-bromophenacyl)-1,4,7,10-tetraazacyclodecane, **9** (bromophenacylcyclen). We hoped to see that the carbonyl, under the strong influence of the proximate zinc(II) ion in cyclen, could become an enolate form by the deprotonation of the adjacent methylene. In this paper, we report a new chemical model for the substrate-bound class II aldolases.

Results and Discussion

Synthesis of Bromophenacylcyclen, 9, and Its Zinc(II) Complex, 10. Bromophenacylcyclen, **9**, was synthesized by the reaction of 1,4,7-tris(*tert*-butoxycarbonyl)cyclen (3Boc-cyclen)[22] with α,4′-dibromoacetophenone in CH_3CN and subsequent

(7) (a) Cooper, S. J.; Leonard, G. A.; McSweeney, S. M.; Thompson, A. W.; Naismith, J. H.; Qamer, S.; Plater, A.; Berry, A.; Hunter, W. N. *Structure* **1996**, *4*, 1303−1315. (b) Blom, N. S.; Tétreault, S.; Coulombe, R.; Sygusch, J. *Nature Struct. Biol.* **1996**, *3*, 856−862.

(8) (a) House H. O. *Modern Synthetic Reactions*, 2nd ed.; Benjamin: Menlo Park, CA, 1972. (b) Fessner, W.-D.; Walter, C. *Top. Curr. Chem.* **1996**, *184*, 97−194. (c) Takayama, S.; McGarvey, G. J.; Wong, C.-H. *Chem. Soc. Rev.* **1997**, *26*, 407−415.

(9) Sato, M.; Ogawa, K.; Akabori, S. *Bull. Chem. Soc. Jpn.* **1957**, *30*, 937−938.

(10) (a) Kimura, E. In *Progress in Inorganic Chemistry*; Karlin, K. D., Ed.; John Wiley & Sons: New York, 1994; Vol. 41, pp 443−491. (b) Kimura, E.; Koike, T. In *Advances in Inorganic Chemistry*; Sykes, A. G., Ed.; Academic Press: New York, 1997; Vol. 44, pp 229−261. (c) Kimura, E.; Koike, T. In *Comprehensive Supramolecular Chemistry*; Reinhoudt, D. N., Ed.; Pregamon: Tokyo, 1996; Vol. 10, pp 429−444.

(11) Kimura, E.; Shiota, T.; Koike, T.; Shiro, M.; Kodama, M. *J. Am. Chem. Soc.* **1990**, *112*, 5805−5811.

(12) Koike, T.; Kimura, E. *J. Am. Chem. Soc.* **1991**, *113*, 8935−8941.

(13) Koike, T.; Kimura, E.; Nakamura, I.; Hashimoto, Y.; Shiro, M. *J. Am. Chem. Soc.* **1992**, *114*, 7338−7345.

(14) Kimura, E.; Shionoya, M.; Hoshino, A.; Ikeda, T.; Yamada, Y. *J. Am. Chem. Soc.* **1992**, *114*, 10134−10137.

(15) Kimura, E.; Nakamura, I.; Koike, T.; Shionoya, M.; Kodama, Y.; Ikeda, T.; Shiro, M. *J. Am. Chem. Soc.* **1994**, *116*, 4764−4771.

(16) Koike, T.; Takamura, M.; Kimura, E. *J. Am. Chem. Soc.* **1994**, *116*, 8443−8449.

(17) Koike, T.; Kajitani, S.; Nakamura, I.; Kimura, E.; Shiro, M. *J. Am. Chem. Soc.* **1995**, *117*, 1210−1219.

(18) Kimura, E.; Kodama, Y.; Koike, T.; Shiro, M. *J. Am. Chem. Soc.* **1995**, *117*, 8304−8311.

(19) Koike, T.; Inoue, M.; Kimura, E.; Shiro, M. *J. Am. Chem. Soc.* **1996**, *118*, 3091−3099.

(20) Koike, T.; Hashimoto, H.; Kimura, E. *J. Am. Chem. Soc.* **1996**, *118*, 10963−10970.

(21) Kimura, E.; Kitamura, H.; Koike, T.; Shiro, M. *J. Am. Chem. Soc.* **1997**, *119*, 10909−10919.

(22) Kimura, E.; Aoki, S.; Koike, T.; Shiro, M. *J. Am. Chem. Soc.* **1997**, *119*, 3068−3076.

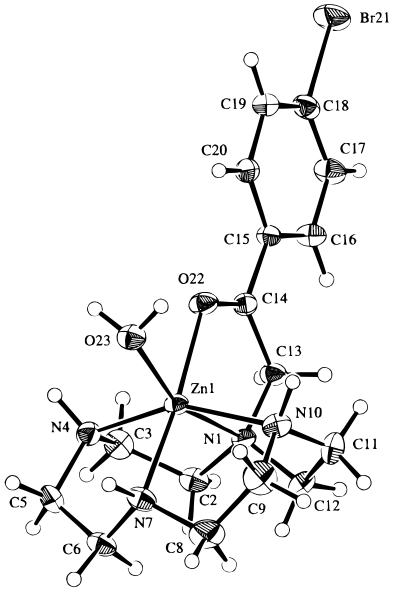

Figure 1. ORTEP drawing (50% probability ellipsoids) of **10**$(ClO_4)_2$. Two perchlorate anions were omitted for clarity. Bond distances (Å): Zn(1)−O(22) 2.159(3), Zn(1)−O(23) 2.130(3), Zn(1)−N(1) 2.238(4), Zn(1)−N(4) 2.143(4), Zn(1)−N(7) 2.135(4), Zn(1)−N(10) 2.163(4). Bond angles (deg): N(1)−Zn(1)−N(4) 82.7(1), N(1)−Zn(1)−N(10) 81.3(1), N(4)−Zn(1)−N(7) 82.3(1), N(7)−Zn(1)−N(10) 82.5(2), O(22)−Zn(1)−O(23) 83.7(1), N(1)−Zn(1)−O(22) 77.0(1).

Scheme 4

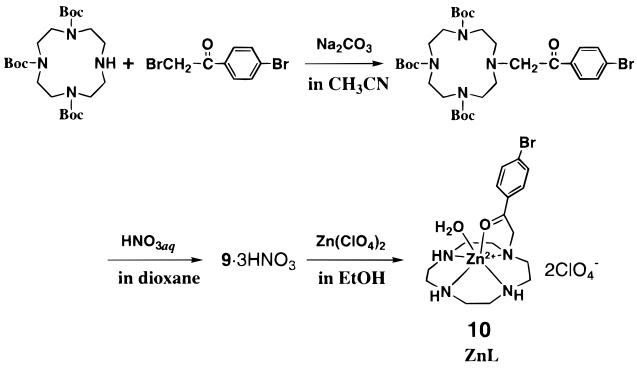

deprotection of *tert*-butoxycarbonyl (Boc) groups with aqueous HNO_3 in 1,4-dioxane (see Scheme 4). The ligand was purified in the form of its $3HNO_3$ salt as colorless needles in 51% yield. The ligand was converted to the acid-free species **9** by extraction with $CHCl_3$ at pH >12. Colorless crystals of the 1:1 zinc(II) complex **10** as its diperchlorate salt were obtained from treatment of **9** with $Zn(ClO_4)_2 \cdot 6H_2O$ in EtOH.

Characterization of the (Bromophenacylcyclen)zinc(II) Complex 10. The carbonyl oxygen-coordinating structure of **10** was established by X-ray analysis, for which colorless needles of **10** were obtained by recrystallization from CH_3CN. Figure 1 shows the ORTEP drawing of **10** with 50% probability thermal ellipsoids. Crystal data and data collection parameters are given in Table 1. The zinc(II) ion is octahedrally coordinated by four nitrogen atoms (N(1), N(4), N(7), and N(10)) of cyclen, the carbonyl oxygen atom O(22), and the water oxygen atom O(23). The Zn−N bond distances are 2.238(4) Å for Zn−N(1), 2.143(4) Å for Zn−N(4), 2.135(4) Å for Zn−N(7), and 2.163(4) Å for Zn−N(10). The Zn−O(22) bond distance is 2.159(3) Å, and the Zn−O(23) bond distance 2.130(3) Å. For comparison, in a five-coordinated, tetragonal-bipyramidal complex **7b** of an alkoxide-pendant cyclen, the Zn−O^- bond distance is 1.91 Å, which is shorter than the Zn−NH bonds (2.06−2.17 Å).[17] Another Zn−O bond distance with a neutral alcohol pendant in **6a** is 1.99 Å, which is also shorter than the Zn−NH bonds (2.10−2.13 Å).[18] The carbonyl stretching frequency (in KBr pellet) shifts from 1699 cm^{-1} for ligand **9** (as a $3HNO_3$ salt with $0.5H_2O$) to 1667 cm^{-1} for **10**$(ClO_4)_2$ (see Figure 2a,b), supporting a reduced C═O character upon coordination with the zinc(II) ion.[23] The UV absorption maximum λ_{max} of **10** occurs at 268 nm (ϵ = 17 600) in 10 mM HEPES buffer (pH 7.5), which is to be compared with λ_{max} 262 nm (ϵ = 17 500) for the free ligand **9** (as mostly a diprotonated form) in the same buffer.

Table 1. Selected Crystallographic Data for **10**$(ClO_4)_2$

empirical formula	$C_{16}H_{27}N_4O_{10}Cl_2BrZn$
fw	651.60
crystal color, habit	colorless, needle
crystal system	monoclinic
space group	$P2_1/n$ (No. 14)
lattice parameters	a = 12.221(8) Å
	b = 11.052(7) Å
	c = 18.194(9) Å
	β = 97.12(3)°
	V = 2438(5) Å^3
	Z = 4
radiation	Mo Kα (λ = 0.710 70 Å), graphite monochromated
μ(Mo Kα)	29.28 cm^{-1}
$2\theta_{max}$	55.0°
no. of reflns measd	4046
refinement	full-matrix least squares
no. of observns	2838
residuals: R; R_w	0.041; 0.046

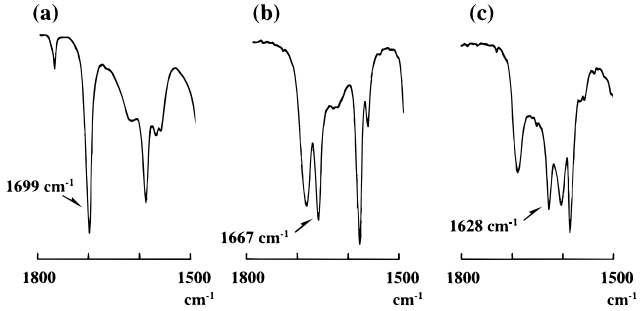

Figure 2. Comparison of IR spectra in the $\nu_{C=O}$ region (KBr pellet): (a) **9**·$3HNO_3 \cdot 0.5H_2O$; (b) **10**$(ClO_4)_2$; (c) **12**(ClO_4).

Protonation and Zinc(II) Complexation Constants of Bromophenacylcyclen, 9. The protonation constants (K_n) of bromophenacylcyclen, **9** (HL), were determined by potentiometric pH titrations of **9**·$3HNO_3$ (1.0 mM) using 0.10 M NaOH with I = 0.10 ($NaNO_3$) at 25 °C. A typical pH titration curve is shown in Figure 3a. The titration data were analyzed for equilibria 1, where a_{H^+} is the activity of H^+. Table 2 summarizes

$$H_{n-1}L^{(n-1)+} + H^+ \rightleftarrows H_nL^{n+} \qquad K_n = [H_nL]/[H_{n-1}L]a_{H^+} \tag{1}$$

the results in comparison with the reference values. The K_1 and K_2 values of **9** (the ligand of **10**) are extremely large with respect to K_3 values, which are roughly the same as those of cyclen ($\log K_1$ = 11.04, $\log K_2$ = 9.86, $\log K_3$ <2, $\log K_4$ <2)[17] and its homologues (see Table 2). Deprotonation of the active methylene group was not observed at *eq*(OH^-) > 3 in **9**.

The 1:1 zinc(II) complexation equilibria were determined by the potentiometric pH titration of **9**·$3HNO_3$ (1.0 mM) in the presence of an equimolar amount of the zinc(II) ion with I =

(23) The new peak at 1690 cm^{-1} for **10**$(ClO_4)_2$ and **12**(ClO_4) is assigned to HN(cyclen)−Zn, which always appears in Zn^{2+}−cyclen homologues.

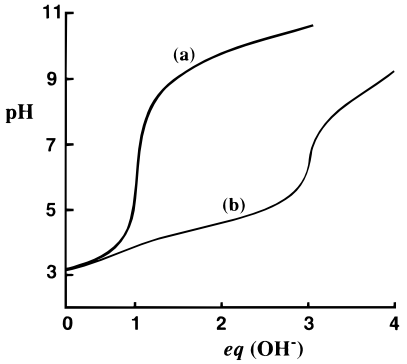

Figure 3. Typical pH titration curves for bromophenacylcyclen, **9**, at 25 °C with $I = 0.10$ ($NaNO_3$): (a) 1.0 mM **9**·3HNO_3; (b) (a) + 1.0 mM $ZnSO_4$.

Table 2. Comparison of Ligand Protonation Constants (K_n),[a] Zinc(II) Complexation Constants (K(ZnL)),[b] Deprotonation Constants (pK_a),[c] and Anion Affinity Constants ($K(A^-)$)[d] at 25 °C with $I = 0.10$ ($NaClO_4$)

	10	**6a**[g]	**15**[h]
log K_1	10.89 ± 0.03	10.72	10.9
log K_2	9.34 ± 0.03	9.28	9.7
log K_3	<2	<2	<2
log K_4	<2	<2	<2
log K(ZnL)	14.1 ± 0.1	13.8	15.1
pK_a at 25 °C	8.41 ± 0.03	7.60	7.68
pK_a at 35 °C	8.20 ± 0.03	7.41	7.50
log $K(OH^-)$	4.9 ± 0.1	6.2	6.1
log $K(SCN^-)$	1.6 ± 0.1[e]	2.0	2.4
log $K(NPP^{2-})$	2.6 ± 0.1[f]	3.0	3.3

[a] $K_n = [H_nL]/[H_{n-1}L]a_{H^+}$ (M^{-1}). [b] $K(ZnL) = [ZnL]/[Zn][L]$ (M^{-1}). [c] $K_a = [ZnH_{-1}L$ and $ZnL-OH^-]a_{H^+}/[ZnL]$ (M). [d] $K(A^-) = [ZnL\text{-}A^-]/[ZnL][A^-]$ (M^{-1}); $A^- = OH^-$, SCN^-, and NPP^{2-}. [e] Determined with 10, 20, and 50 mM SCN^- and 1.0 mM **10**. [f] Determined with 2.0, 5.0, and 10 mM NPP^{2-} and 1.0 mM **10**. [g] From ref 17. [h] From ref 24.

Scheme 5

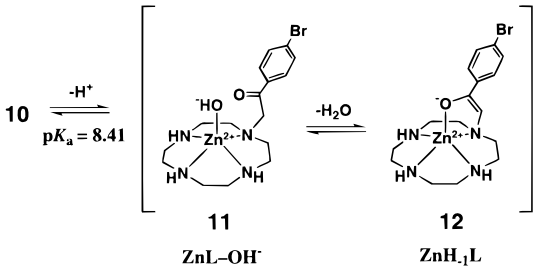

0.10 ($NaClO_4$) at 25.0 °C (Figure 3b). The titration curve revealed two distinct equilibria: the first is the ZnL complex formation until $eq(OH^-) = 3$ (see eq 2),

$$Zn^{2+} + L \rightleftarrows ZnL \qquad K(ZnL) = [ZnL]/[L][Zn^{2+}] \quad (2)$$

$$ZnL \rightleftarrows ZnH_{-1}L \text{ (or } ZnL-OH^-) + H^+$$

$$K_a = [ZnH_{-1}L]a_{H^+}/[ZnL] \quad (3)$$

and the second ($3 < eq(OH^-) < 4$) is deprotonation from ZnL (see eq 3). Up to $eq(OH^-) = 3$, the equilibration was extremely slow, so that we had to wait more than 2 h for each titration point. For the ZnL complex in aqueous solution, the structure **10** is assignable. On the other hand, the following deprotonation at $3 < eq(OH^-) < 4$ was fast enough to attain equilibrium within 5 min at each titration point. The deprotonation equilibrium can be drawn as shown in Scheme 5. For the deprotonated complex, either the hydroxide-bound $ZnL-OH^-$ complex **11** or the enolate-bound $ZnH_{-1}L$ complex **12** may be considered.

Scheme 6

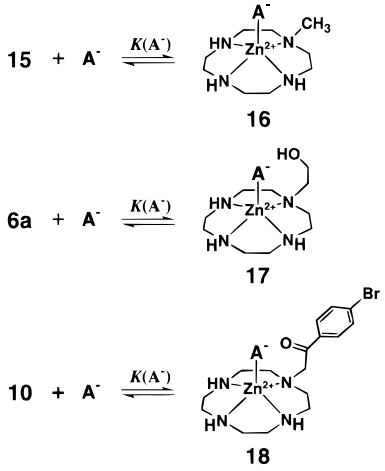

All of the calculated values for bromophenacylcyclen are summarized in Table 2, to compare with the relevant values for ethanol-pendant cyclen **13** and methylcyclen **14**. The pK_a

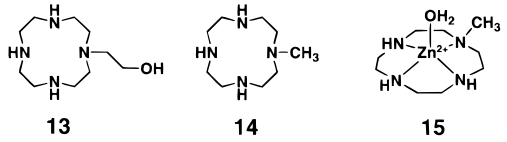

value of 8.41 at 25 °C is higher than those of 7.60 for **6a**,[17] 7.51 for **7a**,[18] and 7.68 for the Zn^{2+}-bound water in **15**.[24] We have assigned the structure of the deprotonated species (in water) to be a mixture of **11** and **12** rather than either of the single species, as discussed subsequently.

Competitive Anion Binding to the (Bromophenacylcyclen)zinc(II) Complex 10. In the Zn^{2+}−methylcyclen complex **15**, various anions ($A^- = SCN^-$, 4-nitrophenyl phosphate, or OH^-) easily replaced the apical H_2O to yield the 1:1 $ZnL-A^-$ complexes **16** (see Scheme 6).[18] These anions competitively replaced the pendant alcohol (a neutral donor) in **6a** to yield the $ZnL-A^-$ complexes **17**.[18] To see analogous anion binding in the present bromophenacylcyclen complex **10** (to yield **18**) (see Scheme 6), we conducted the potentiometric pH titration of ZnL, **10**, in the presence of excess amounts of SCN^- and 4-nitrophenyl phosphate (NPP^{2-}) at 25 °C with $I = 0.10$ ($NaClO_4$). The 1:1 affinity constants ($K(A^-) = [ZnL-A^-]/[ZnL][A^-]$ M^{-1}) were calculated in the same fashion as previously described for **16** and **17**. The log $K(A^-)$ values for **18** are 1.6 ($A^- = SCN^-$) and 2.6 ($A^- = NPP^{2-}$), which are smaller than the corresponding values of 2.0 and 3.0 for **17**, which in turn are smaller than 2.4 and 3.3 for **16** (see Table 2). The stronger interaction of the present carbonyl oxygen than the alcoholic OH or external H_2O with the zinc(II) ion would be responsible for the weakest anion binding for **10**. This fact is compatible with the weakest binding of OH^- to the zinc(II) ion in **18** (cf. $K(OH^-) = 4.9$ for **10**, 6.2 for **6a**, and 6.1 for **15**).

Isolation and Characterization of the Enolate-Bound Complex $ZnH_{-1}L$, 12. One of the deprotonated species, the enolate-bound complex **12**, was independently isolated as an analytically pure perchlolate salt by treating **10** with an equivalent amount of NaOMe in CH_3CN. To our knowledge, this is the first isolation of the enolate-bound zinc(II) complex. The UV absorption spectrum of **12** (λ_{max} 296 nm, $\epsilon = 7900$) is characteristically different from that of **10** (λ_{max} 268 nm, $\epsilon =$

(24) Shionoya, M.; Ikeda, T.; Kimura, E.; Shiro, M. *J. Am. Chem. Soc.* **1994**, *116*, 3848−3859.

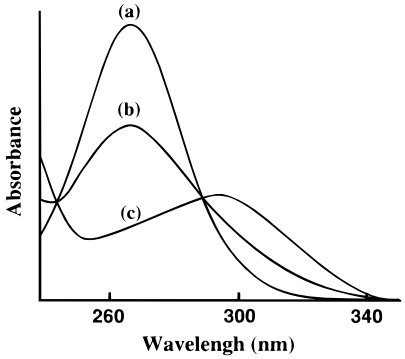

Figure 4. UV absorption spectra of **10** at 25 °C in CH_3CN: (a) 0.50 mM **10**; (b) (a) + 0.25 mM DBU; (c) (a) + 0.50 mM DBU, an identical spectrum obtained for **12** in CH_3CN.

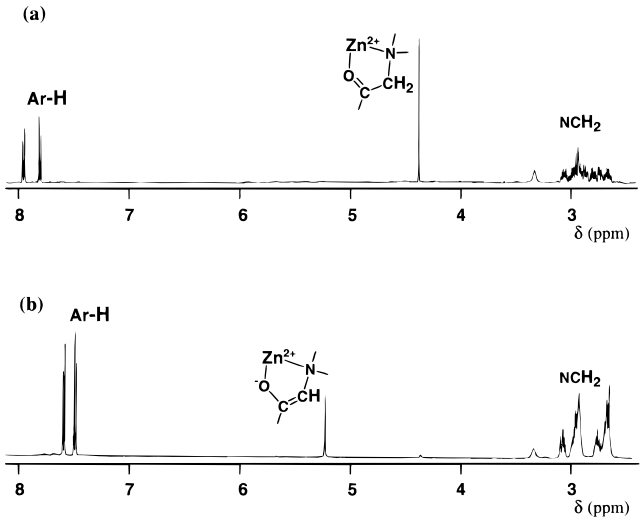

Figure 5. Comparison of ^{1}H NMR spectra at 35 °C in CD_3CN: (a) 10 mM **10**$(ClO_4)_2$; (b) 10 mM **12**(ClO_4).

18 700) in acetonitrile. The IR spectrum showed an enolate band at 1628 cm^{-1} (see Figure 2c).[23] The remarkable UV spectral change in going from **10** to **12** was seen in the titration of **10** (0.5 mM) with 1,8-diazabicyclo[5.4.0]-7-undecene (DBU) (0−0.5 mM) in CH_3CN (Figure 4). Comparison of the ^{1}H NMR spectrum of **12** with that of **10** in CD_3CN (Figure 5) showed upfield shifts for the two kinds of aromatic H's (δ 7.80 and 7.93 → 7.45 and 7.56) and a low-field shift for $-CH_2-C{=}O$ (δ 4.38) → $-CH{=}C-O^-$ (δ 5.21). The ^{13}C NMR spectra (by nondecoupled DEPT method) showed a triplet (J_{CH} = 135 Hz, due to coupling $-CH_2-$) at δ = 62 for the carbon adjacent to the carbonyl in **10**, which is changed to a doublet (J_{CH} = 177 Hz, due to coupling $=CH-$) at δ = 106 for the enolate carbon in **12**. These NMR data in CD_3CN undoubtedly fit the enolate structure **12** but not the other form **11**.

NMR and UV Spectrophotometric Study of ZnL, 10, at Various pHs. To assign the correct structure(s) **11** and/or **12** for the deprotonated species in aqueous solution, we recorded ^{1}H and ^{13}C NMR spectra of **10** at pH 6.7 (below the pK_a value of 8.41) and 9.4 (above the pK_a value) in a 10% (v/v) D_2O/H_2O solution (see Scheme 7). At pH 6.7, the NMR spectra of **10** showed one carbonyl carbon signal at δ = 203 and its adjacent methylene carbon signal as a triplet at δ = 64 with J_{CH} = 135 Hz and two aromatic proton signals as doublets at δ = 7.87 and 8.02 with J = 8.9 Hz. These data agree with the single structure ZnL, **10**. As anticipated, the methylene H atoms of **10** were rapidly displaced by D at physiological pH. The first-order rate constants (at 25 °C) for NCH_2CO → NCHDCO in pD 7.0 and 7.2 MOPS (20 mM) buffer in 10% (v/v) CD_3CN/D_2O were determined to be $(2.8 \pm 0.3) \times 10^{-2}$ and $(4.6 \pm 0.5) \times 10^{-2}$ min^{-1}, respectively.[25] In other words, the half-lives are 25 min (pD 7.0) and 15 min (pD 7.2). At pD 7.5, the H−D exchange occurred within a few minutes, so that we could not determine the rate. For comparison, the H−D replacement for the free ligand **9** in pD 7.0 MOPS buffer (D_2O only) (where **9** is mostly in a diprotonated form) was very slow. Its first-order rate constant (25 °C) was $(2.7 \pm 0.3) \times 10^{-4}$ min^{-1} (i.e., the half-life = 43 h).[25] Thus, the zinc(II) ion accelerates enolization by 100 times relative to the diprotonated form.

Scheme 7

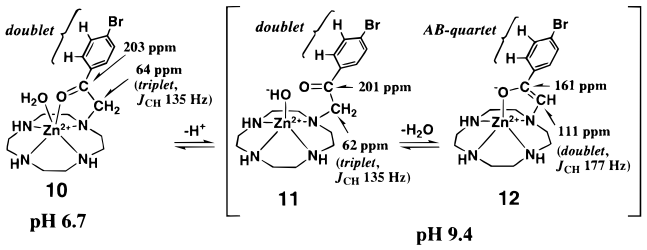

The ^{13}C NMR spectra at pH 9.4 showed two distinct sets of species. One spectral set almost parallels that for **10**: carbonyl carbon signal at δ = 201 and its adjacent methylene carbon as a triplet at δ = 62 with J_{CH} = 135 Hz; two aromatic protons as doublets at δ = 7.76 and 7.89 with J = 8.5 Hz. These data are compatible with the OH^--bound structure **11**. The other spectral set differed significantly, which supports the enolate-form structure **12** (as earlier measured in CD_3CN): $=C-O^-$ carbon signal at δ = 161, its adjacent methylene carbon as a doublet at δ = 111 with J_{CH} = 177 Hz, and the aromatic protons in an AB quartet at δ = 7.57. The ^{13}C NMR spectral change for the methylene carbon in aqueous solution parallels the change in the above CD_3CN solution. The concentration ratios of [**12**] to [**11**] in 10% (v/v) D_2O/H_2O solution were calculated by comparison of the intensities of the aromatic protons to be 0.27, 0.30, and 0.34 at 15, 25, and 35 °C, respectively, with I = 0.10 ($NaClO_4$). These ratios did not change irrespective of the solution pH (up to 12). The van't Hoff plot of the equilibrium constant for **11** ⇄ **12** against $1/T$ (K^{-1}) gives a linear line which affords estimated values of $\Delta G = 3.0 \pm 0.3$ kJ mol^{-1}, $\Delta H = 8.7 \pm 0.3$ kJ mol^{-1}, and $\Delta S = 19 \pm 2$ J mol^{-1} K^{-1} at 25 °C. Although the conversion from the keto form **11** to the enolate form **12** is endothermic, the positive ΔS compensates for the enthalpy loss. The separately isolated **12**, which gave a sole NMR spectrum for **12** in CD_3CN, yielded a mixture of **11** and **12** in the same ratio in aqueous solution. However, in 50% (v/v) CD_3CN/H_2O solution, the ratio of [**12**] to [**11**] greatly increased to 1.50 at 35 °C.

The UV spectrophotometric titration of **10** (0.5 mM) in aqueous solution with NaOH (0−0.5 mM) (Figure 6) allowed us to calculate the pK_a value of 8.4, which is the same as the pK_a value determined by the potentiometric pH titration. The UV spectrum at pH 9.4 in aqueous solution fits to a combination of hypothetical spectra of pure **11** (λ_{max} 262 nm, ϵ = 18 600) (Figure 6d) and **12** (λ_{max} 296 nm, ϵ = 7900) (Figure 6e) in a 3:1 ratio.

Basicity and Nucleophilicity of $Zn^{2+}-OH^-$ in 11. Our previous studies well demonstrated that the Zn^{2+}-bound hydroxides can act as general bases[24,26,27] and nucleophiles.[10−20] The hydroxide in **11** has also been shown to behave similarly. For the basic character, we found that the $Zn^{2+}-OH^-$ complex

(25) A singlet at δ 4.55 (NCH_2CO) is replaced by an upfield singlet at δ 4.52 (NCHDCO) in **10**. Also, a singlet at δ 4.38 (NCH_2CO) is replaced by an upfield singlet at δ 4.35 (NCHDCO) in **9** (where **9** is mostly in the diprotonated form $L{\cdot}2H^+$).

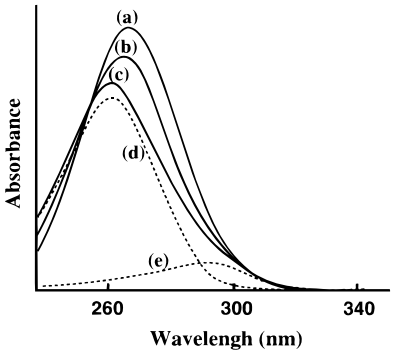

Figure 6. UV absorption spectra at 25 °C in aqueous solution: (a) 0.50 mM **10** (pH 6.7); (b) (a) + 0.25 mM NaOH (pH 8.4); (c) (a) + 0.50 mM NaOH (pH 9.4). Breakdown of the spectrum (c) into two theoretical composites of **11** (d) and **12** (e) in a 3:1 ratio.

Scheme 8

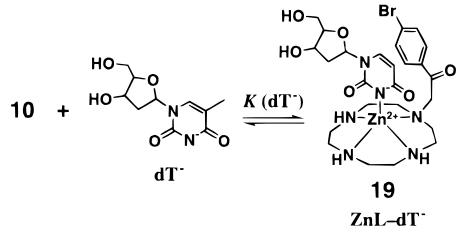

deprotonates thymidine (dT) to an N(3)-deprotonated conjugate base (dT^-) which yielded the 1:1 ternary complex **19** with log $K(dT^-)$ ($=[ZnL-dT^-]/[ZnL][dT^-]$ M^{-1}) of 5.9 ± 0.1 (Scheme 8), to be compared with the log $K(dT^-)$ value of 5.6 for the $(Zn^{2+}-cyclen)-dT^-$ complex. The present value for **19** was obtained by the potentiometric pH titration as described earlier.[26]

As for the nucleophilicity, we have measured the phosphate hydrolysis of bis(4-nitrophenyl) phosphate (BNP^-) by a mixture of **11** and **12** at 35 °C with $I = 0.1$ ($NaClO_4$). The procedure was identical to the one employed for $(Zn^{2+}-cyclen)-OH^-$, **20**, except that here we used Good's buffers (see the Experimental Section).[12] As before, the second-order (each first order in [BNP^-] and [**11** and **12**]) rate constant k_{BNP} was determined to be $(4.3 \pm 0.2) \times 10^{-5}$ M^{-1} s^{-1}, which is on the same order as 2.1×10^{-5} M^{-1} s^{-1} reported for **20**.[12]

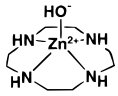

20

Implications of the Present Findings for the Role of Zinc(II) in Class II Aldolases. In the active center of class II aldolases, the acyclic carbonyl form of FBP may not be significantly polarized,[6] while the carbonyl of DHAP is polarized and the enediol (or enediolate) form of DHAP bound to Zn^{2+} is detected in the ^{13}C NMR spectrum.[6] A currently postulated mechanism is as follows.[5b] The first step consists of the binding of the acyclic carbonyl-FBP to the enzyme (not necessarily to Zn^{2+}). Following the abstraction of a proton from the C4 hydroxyl, FBP is cleaved at the C3−C4 bond (see **3**), leading to the formation of (enzyme-bound) G3P and Zn^{2+}-bound enediol(ate) DHAP. After conversion of the Zn^{2+}-bound enediol(ate) DHAP to its keto form, DHAP is released from the enzyme. In the aldolase from *E. coli*, the pK_a value for keto ⇄ enolate DHAP seems to be near 8 (as estimated from the 50% maximum pH by a ^{13}C NMR study),[6] a factor of at least 10^6 down from pK_a value of ca. 14 for free DHAP.[28] Furthermore, it has been suggested that FBP and DHAP when bound to enzymes are unlikely to interact directly with the zinc(II) ion.[6] Meanwhile, the enediolate stabilization by chelate coordination to Zn^{2+} (see **1**) was proposed from its analogy to the X-ray structure of a Zn^{2+} complex of phosphoglycolohydroxamate, an inhibitor in aldolase **21**.[5b] Altogether, a coherent mechanistic picture involving Zn^{2+} is hardly drawn from these enzymatic studies.

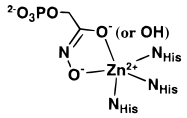

21

The present findings by our model study, in connection with these class II aldolase functions, have disclosed the following new intrinsic chemical properties of zinc(II) ions: (1) The zinc(II) ion can bind to a carbonyl oxygen. The ^{13}C NMR signal of the Zn^{2+}-bound carbonyl appeared at $\delta = 203$ for **10**, almost the same chemical shift as $\delta = 204$ of the free ligand **9**·$2H^+$ carbonyl in D_2O. These are to be compared with the reported chemical shift at $\delta = 215$ for carbonyl carbon (C2) in keto-FBP in aldolase (see **22**).[6] (2) The pK_a values of acetone (19.2)[29] and acetophenone (18.3)[30] in aqueous solution were previously reported. The zinc(II) ion can dramatically facilitate enolate formation of the acetophenone moiety in **10** (pK_a = 8.4). This discovery well accounts for the reported pH-dependent appearance of the enediolate form of DHAP only in the presence of Zn^{2+} in the enzyme, by which the enolate form reached a maximum at pH 9 and a 50% maximum at pH 8.[6] The DHAP resonance ($\delta = 213$) of **2** shifted down to $\delta = 147$ due to the enediolate-DHAP complexation with Zn^{2+} (see **1**).[6] Our free carbonyl ($\delta = 204$) in **9**·$2H^+$ shifted down to $\delta = 161$ in **12** upon the enolate complexation. (3) In addition to thermodynamically stabilizing the enolate form, Zn^{2+} kinetically increases the enolization rate. While acetophenone hardly undergoes the H−D exchange at the methylene group at pD 7.0 in D_2O solution, the acetophenone moiety in **10** is displaced with a half-life of 25 min. Under the same conditions, ligand **9** undergoes the exchange with a half-life of 43 h. Some acceleration is due to the effect of two protons in the cyclen. (4) The competitive binding of the carbonyl oxygen and anions with our model (see Scheme 6) illustrates the feasible replacement of Glu(73) by the carbonyls of the substrates DHAP and FBP in the enzyme.[5a] (5) In the presence of waters near Zn^{2+}, the OH^- formation instead of the enolate formation occurs competitively. This is probably the case in the hydrated Zn^{2+} environment of aldolases, too. This OH^- may act as a general base catalyst, as demonstrated by our model. (6) The equilibrium between **11** and **12** with our model may allow us to consider a new mechanistic picture (see Scheme 9), where, for the reverse aldol condensation, the C4-hydroxyl hydrogen of FBP is deprotonated by the $Zn^{2+}-OH^-$ in **22** (as previously found for **6a** ⇄ **6b** ⇄ **6c**),[17] which immediately drives the retroaldol reaction to produce the stable enediolate DHAP−Zn^{2+} complex

(26) Shionoya, M.; Kimura, E.; Shiro, M. *J. Am. Chem. Soc.* **1993**, *115*, 6730−6737.
(27) Koike, T.; Gotoh, T.; Aoki, S.; Kimura, E.; Shiro, M. *Inorg. Chim. Acta* **1998**, *270*, 424−432.
(28) Alagona, G.; Desmeules, P.; Ghio, C.; Kollman, P. A. *J. Am. Chem. Soc.* **1984**, *106*, 3623−3632.
(29) Chiang, Y.; Kresge, A. J.; Tang, Y. S.; Wirz, J. *J. Am. Chem. Soc.* **1984**, *106*, 460−462.
(30) Chiang, Y.; Kresge, A. J.; Wirz, J. *J. Am. Chem. Soc.* **1984**, *106*, 6392−6395.

Scheme 9

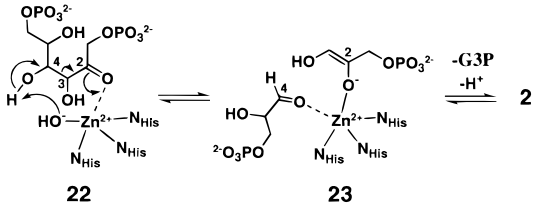

(**23**) and then **2** after protonation with pK_a ca. 8. In an earlier proposal,[5a] Tyr(113) was considered to act as a general base to deprotonate the C4-OH. The occurrence of the phenolate anion under physiological conditions is unlikely, in view of its pK_a value of ca. 10.

Conclusion

The new carbonyl-bound Zn^{2+} complex **10** was demonstrated to be the first good model that serves to elucidate the role of Zn^{2+} in the class II aldolases. The deprotonation of the Zn^{2+}-bound carbonyl occurred with a pK_a value of 8.41 (at 25 °C), and one of the resulting products, the enolate-bound complex **12**, was separately isolated in CH_3CN for characterization. Thus, the Zn^{2+} ion demonstrated a thermodynamic effect to raise the acidity of the carbonyl methylene (ordinary pK_a ca. 19 in aqueous solution) by orders of 10. This is an extraordinarily large pK_a shift. In an earlier organic model for enolase, the acidity of 1,3-diketones increased only by 1 pK_a unit in CH_3CN.[31] Our model implicates the feasibility of the enediolate DHAP−Zn^{2+} complex **1** in the class II aldolases. The methylene hydrogen atoms adjacent to the Zn^{2+}-bound carbonyl in **10** were kinetically activated, as shown by the rapid H−D exchange by deuterium in neutral D_2O; its half-life was 25 min at 25 °C in pD 7.0 MOPS buffer. In another organic enolase model using protonated macrocyclic polyamines, the H−D exchange of malonate ions was accelerated by factors of 10^3−10^5 in pD 7 D_2O.[32]

The deprotonation from **10** competitively yielded the isomeric Zn^{2+}−OH^- complex **11** in the **12**:**11** equilibrium ratio of 1:3 regardless of the aqueous solution pH at 25 °C. The Zn^{2+}-bound hydroxide anion **11** acted as a general base to deprotonate the imide hydrogen of thymidine. This fact suggests that such a Zn^{2+}-bound hydroxide anion may also be produced in the active center of class II aldolases, which then acts to deprotonate the C_4-OH of fructose, a substrate to initiate the reverse aldol reaction. Under more anhydrous conditions, the equilibrium shifted to the enolate-bound complex **12**, and in pure CH_3CN solution, only **12** was formed. The present discovery that, in the presence of Zn^{2+}, enolates can be generated near neutral pH would be useful information in exploring more refined Zn^{2+}-catalyzed aldol reactions and other synthetic chemistry in aqueous solution.

Experimental Section

General Information. All reagents and solvents used were purchased at the highest commercial quality and used without further purification. Anhydrous acetonitrile (CH_3CN) was distilled from calcium hydride. The Good's buffers (Dojindo) were commercially available: MOPS (3-(*N*-morpholino)propanesulfonic acid, pK_a = 7.2), HEPES (*N*-(2-hydroxyethyl)piperazine-*N*″-2-ethanesulfonic acid, pK_a = 7.5), TAPS (*N*-(tris(hydroxymethyl)methyl)amino)-3-propanesulfonic acid, pK_a = 8.4), CHES (2-(cyclohexylamino)ethanesulfonic acid, pK_a = 9.5). Sodium bis(4-nitrophenyl) phosphate was crystallized from an aqueous solution of bis(4-nitrophenyl)phospholic acid (BNP) and equimolar NaOH. All aqueous solutions were prepared using deionized and distilled water. UV spectra were recorded on a Hitachi U-3500 spectrophotometer equipped with a temperature controller unit with I = 0.10 ($NaClO_4$) at 25.0 ± 0.1 °C. IR spectra were recorded on a Shimadzu FTIR-4200 spectrophotometer at room temperature. ^{1}H (500 MHz) and ^{13}C (125 MHz) NMR spectra at 35.0 ± 0.1 °C were recorded on a JEOL LA500 spectrometer. 3-(Trimethylsilyl)propionic-*2,2,3,3-d*$_4$ acid sodium salt in D_2O and tetramethylsilane in CD_3CN were used as internal references for ^{1}H and ^{13}C NMR measurements. The pD values in D_2O were corrected for a deuterium isotope effect using pD = (pH-meter reading) + 0.40.[33] The ^{1}H NMR and ^{13}C NMR assignments were accomplished by 1D (^{1}H and ^{13}C) and 2D (HMQC and HMBC) experiments. Elemental analyses were performed on a Perkin-Elmer CHN 2400 analyzer. Thin-layer (TLC) and silica gel column chromatographies were performed using a Merck 5554 (silica gel) TLC plate and Fuji Silysia Chemical FL-100D, respectively.

Synthesis of the 1-(4-Bromophenacyl)-1,4,7,10-tetraazacyclododecane Trinitric Acid Salt, 9·3HNO$_3$·0.5H$_2$O. A solution of α,4′-dibromoacetophenone (2.36 g, 8.50 mmol) and 1,4,7-tris(*tert*-butyloxycarbonyl)-1,4,7,10-tetraazacyclododecane (3.98 g, 8.44 mmol)[22] in CH_3CN (40 mL) was stirred in the presence of Na_2CO_3 (0.898 g, 8.47 mmol) at 80 °C under an argon atmosphere for 1 day. After insoluble inorganic salts had been filtered off, the filtrate was concentrated under reduced pressure. The residue was purified by silica gel column chromatography (eluted by hexanes/AcOEt). After evaporation of the solvent, the residue was dissolved in dioxane (50 mL). To the dioxane solution was slowly added 61% aqueous HNO_3 (50 mL). The reaction mixture was stirred for 4 h at room temperature. After the solvent had been evaporated, the residue was crystallized from H_2O to obtain colorless needles of **9**·3HNO$_3$·0.5H$_2$O (2.44 g, 51.0% yield): IR (KBr pellet) 3450, 3044, 2652, 1763, 1699 (CO), 1588, 1470, 1385, 1219, 1073, 970, 825, 772 cm^{-1}; ^{1}H NMR (D_2O) δ 3.04−3.21 (16H, br, N−CH_2), 4.36 (2H, s, HC-13), 7.75 (2H, d, J = 8.5 Hz, C-17,19), 7.88 (2H, d, J = 8.5 Hz, C-16,20); ^{13}C NMR (D_2O) δ 44.97, 45.56, 47.34, 52.74 (C-2,12) 62.39 (C-13), 132.16 (C15), 132.52 (C-16,20), 135.12 (C-17,19), 136.28 (C-18), 203.51(C-14). Anal. Calcd for $C_{16}H_{29}N_7O_{10.5}Br$: C, 33.87; H, 5.15; N, 17.28. Found: C, 33.97; H, 5.12; N, 17.43.

Synthesis of the Zinc(II) Complex with 9 (10(ClO$_4$)$_2$). An aqueous solution (40 mL) of **9**·3HNO$_3$·0.5H$_2$O (1.13 g, 2.00 mmol) was added to a 1 M NaOH aqueous solution (10 mL). The solution was extracted with $CHCl_3$ (50 mL × 5). After the combined organic layers had been dried over anhydrous Na_2SO_4, the solvent was evaporated to obtain **9** as a pale yellow oil. To an EtOH solution (10 mL) of **9** was added $Zn(ClO_4)_2$·6H_2O (0.744 g, 2.00 mmol). The solution was stirred at room temperature for 2 h. After the solvent was evaporated, the residue was crystallized from CH_3CN to obtain colorless needles of **10**$(ClO_4)_2$ (1.06 g, 81.6% yield): IR (KBr pellet) 3416, 3291, 2920, 1690 (NH−Zn), 1667 (CO), 1586, 1456, 1400, 1240, 1144, 1117, 1088, 968, 812, 625 cm^{-1}; ^{1}H NMR (CD_3CN) δ 2.62−3.08 (16H, m, N−CH_2), 4.38 (2H, s, HC-13), 7.80 (2H, d, J = 8.5 Hz, C-17,19), 7.93 (2H, d, J = 8.5 Hz, C-16,20); ^{13}C NMR (CD_3CN) δ 44.99, 45.55, 47.08, 55.26 (C-2, 12), 62.00 (t, J_{CH} = 135 Hz, C-13), 131.38 (C-15), 131.65 (C-16,20), 133.54 (C-17,19), 133.63 (C-18), 201.30 (C-14). Anal. Calcd for $C_{16}H_{27}N_4O_{10}Cl_2BrZn$: C, 29.49; H, 4.18; N, 8.60. Found: C, 29.62; H, 4.14; N, 8.60.

The ^{1}H and ^{13}C NMR spectra of the (bromophenacylcyclen)zinc(II) complex **10** at pH 6.7 and 9.4 (OH^--bound complex **11** and enolate-bound complex **12**) in 10% (v/v) D_2O/H_2O solution were assigned as follows. Numbering of the carbons corresponds to the X-ray structure numbering. The methylene peaks adjacent to the carbonyl in **10** and **11** and the vinyl CH peak in **12** were not assigned, since these peaks overlapped with the H_2O peak. **10** at pH 6.7: ^{1}H NMR δ 2.82−3.18 (16H, m, N−CH_2), 7.87 (2H, d, J = 8.9 Hz, HC-17,19), 8.02 (2H, d, J = 8.9 Hz, HC-16,20); ^{13}C NMR δ 46.59, 47.19, 48.68, 56.73 (C-2,12), 63.61 (t, J_{CH} = 135 Hz, C-13), 133.04 (C-15), 133.22 (C-16,-20), 135.20 (C-17,19), 135.31 (C-18), 203.10 (C-14). Data for **10** at pH 9.4 are as follows. OH^--bound complex **11**: ^{1}H NMR δ 7.76 (1.5H,

(31) Kelly-Rowley, A. M.; Lynch, V. M.; Ansyln, E. V. *J. Am. Chem. Soc.* **1995**, *117*, 3438−3447.

(32) Fenniri, H.; Lehn, J.-M.; Marquis-Rigault, A. *Angew. Chem., Int. Ed. Engl.* **1996**, *35*, 337−339.

(33) Glasoe, P. K.; Long, F. A. *J. Phys. Chem.* **1960**, *64*, 188−190.

d, J = 8.5 Hz, HC-17,19), 7.89 (1.5H, d, J = 8.5 Hz, HC-16,20); ^{13}C NMR δ 45.67, 46.48, 47.66, 57.51 (C-2, 12), 61.75 (t, J_{CH} = 135 Hz, C-13), 131.83 (C-15), 132.35 (C-16,20), 134.98 (C-17,19), 136.50 (C-18), 200.78 (C-14). Enolate-bound complex **12**: ^{1}H NMR δ 7.57 (1H, AB quartet, HC-16,17,19,20); ^{13}C NMR δ 48.25, 48.37, 48.81, 54.41 (C-2, 12), 110.89 (d, J_{CH} = 177 Hz, C-13), 124.33 (C-15), 129.93 (C-16,20), 134.12 (C-17,19), 139.76 (C-18), 161.21 (C-14).

Preparation of the Enolate-Bound Zinc(II) Complex (12(ClO$_4$)). To a solution of **10**(ClO$_4$)$_2$ (330 mg, 0.5 mmol) in CH$_3$CN (5 mL) was added 0.5 mL of 1 M NaOMe in MeOH. After the solvent was evaporated, the residue was crystallized from CH$_3$CN/MeOH to obtain colorless prisms of **12**(ClO$_4$) (249 mg, 89% yield): IR (KBr pellet) 3480, 3333, 2923, 1690 (NH−Zn), 1628 (enolate), 1605, 1586, 1482, 1456, 1397, 1350, 1144, 1119, 1090, 627 cm^{-1}; ^{1}H NMR (CD$_3$CN) δ 2.60−3.08 (16H, m, N−CH$_2$), 5.21 (1H, s, HC-13), 7.45 (2H, d, J = 8.9 Hz, HC-17,19), 7.56 (2H, d, J = 8.6 Hz, HC-16,20); ^{13}C NMR (CD$_3$CN) δ 45.39, 45.80, 46.70, 55.42 (C-2, 12), 106.10 (d, J_{CH} = 177 Hz, C-13), 121.84 (C-15), 128.40 (C-16,20), 131.93 (C-17,19), 140.21 (C-18), 161.76 (C-14). Anal. Calcd for C$_{16}$H$_{24}$N$_4$O$_5$ClBrZn: C, 36.05; H, 4.54; N, 10.51. Found: C, 36.05; H, 4.72; N, 10.39.

Potentiometric pH Titration. A titrant solution of 0.100 M NaOH was prepared by dilution of an aqueous solution of 10 M NaOH (Merk 6495) with decarbonated water below 5 °C, where the contamination of Na$_2$CO$_3$ is less than 0.5 mM. A glass pH electrode, Orion Research ROSS electrode model 81-02, was used, which is one of the highest quality electrodes, providing a pH stability within 0.01 pH unit and a straight relationship between pH response (mV) and log a_{H^+} in the pH range 2−12. The electrode system with a pH meter (DKK Corp., IOL-40) was daily calibrated as follows: An aqueous solution (50 mL) containing 4.00 mM HCl and 96 mM NaNO$_3$ (I = 0.10) was prepared under an argon atmosphere (>99.999% purity) at 25.0 ± 0.1 and 35.0 ± 0.1 °C; then the first pH value (pH$_1$) was read. After 4.00 mL of 0.100 M NaOH had been added to the acidic solution, the second pH value (pH$_2$) was read. The theoretical pH values corresponding to pH$_1$ and pH$_2$ are calculated to be pH$_1'$ = 2.481, 2.483 and pH$_2'$ = 11.447, 11.128, respectively. The used values of K_w' (=[H$^+$][OH$^-$]) and f_{H^+} (=a_{H^+}/[H$^+$]) were $10^{-13.79}$ and 0.825 at 25 °C and $10^{-13.48}$ and 0.823 at 35 °C, respectively. The correct pH values (pH = −log a_{H^+}) can be obtained using the following equations: a = (pH$_2'$ − pH$_1'$)/(pH$_2$ − pH$_1$); b = pH$_2'$ − a × pH$_2$; pH = a × (pH-meter reading) + b. The calibration method provides an experimental confidence limit of ±0.01 pH unit.

The potentiometric pH titration of **9** (1.0 mM) was carried out with I = 0.10 (NaNO$_3$), and at least two independent titrations were performed. Protonation constants (K_n' = [H$_n$L]/[H$_{n-1}$L][H$^+$]) of **9**, the deprotonation constant (pK_a' = log([**10**]/[**11** + **12**][H$^+$])) of **10**, the metal complexation constant (K(ZnL) = [ZnL]/[Zn][L]), and the thymidine anion (dT$^-$) complexation constant (K(ZnL−dT$^-$) = [ZnL−dT$^-$]/[ZnL][dT$^-$]) were determined by means of the pH-titration program BEST.[34] The mixed constants (K_n = [H$_n$L]/[H$_{n-1}$L]a_{H^+} and pK_a = log([**10**]/[**11** + **12**]a_{H^+})) are derived from K_n' and pK_a' by [H$^+$] = a_{H^+}/f_{H^+}. Anion affinity constants K(A$^-$) (=[ZnL−A$^-$]/[ZnL][A$^-$]) were determined from pH titration data at 3 < eq(OH$^-$) < 4 in the presence of excess amounts of anions (SCN$^-$, 4-nitrophenyl phosphate) as previously described.[11] The hydroxide anion affinity constant K(OH$^-$) of **10** was calculated from pK_a', the **11**:**12** ratio, and K_w'.

Kinetics of the Phosphodiester Cleavage Reaction in Aqueous Solution. The phosphodiester cleavage reaction (i.e., the 4-nitrophenolate release reaction) rate for bis(4-nitrophenyl) phosphate (BNP$^-$) was measured by an initial-slope method (following the increase in 400 nm absorption of released 4-nitrophenolate) in aqueous solution at 35.0 ± 0.5 °C. Buffer solutions containing 20 mM Good's buffers (HEPES, pH 7.6; TAPS, pH 8.2; CHES, pH 9.3) were used, and the ionic strength was adjusted to 0.10 with NaClO$_4$. For the initial rate determination, the following typical procedure was employed: After BNP$^-$ (5.0 mM) and **10** (1.0 mM) had been mixed in the buffer solution, the UV absorption increase was immediately recorded until ca. 0.3% formation of 4-nitrophenolate, where log ϵ values for 4-nitrophenolate were 4.12 (pH 7.6), 4.22 (pH 8.2), and 4.26 (pH 9.3) at 400 nm. The first-order rate constant k_{obsd} (s^{-1}) was calculated from the decay slope (4-nitrophenolate/[BNP$^-$]). The value of k_{obsd}/[total Zn^{2+} complex] gave the second-order rate constant k'_{BNP} (M^{-1} s^{-1}) for BNP$^-$ hydrolysis. The second-order rate constant k_{BNP} was determined from the maximum k'_{BNP} values.

Crystallographic Study of the Zinc Complex 10(ClO$_4$)$_2$. A colorless needle crystal of **10**(ClO$_4$)$_2$ (C$_{16}$H$_{27}$N$_4$O$_{10}$Cl$_2$BrZn, M_r = 651.60), having approximate dimensions 0.35 × 0.05 × 0.02 mm, was mounted in a glass capillary. All measurements were made on a Rigaku RAXIS IV imaging plate area detector with graphite-monochromated Mo Kα radiation (μ = 29.28 cm^{-1}) at 25 ± 1 °C. Indexing was performed from two oscillation images which were exposed for 4 min. A total of 36 oscillation (3.0°) images were collected, each being exposed for 30 min. The crystal-to-detector distance was 105 mm at the detector zero swing position. Readout was performed in the 100 μm pixel mode. The structure was solved by direct methods (SIR 92) and expanded by means of Fourier techniques (DIRDIF 94). All calculations were performed with the teXsan crystallographic software package developed by the Molecular Structure Corp. (1985, 1992).

Acknowledgment. We are grateful to the Ministry of Education, Science, and Culture of Japan for financial support through a Grant-in-Aid for the Priority Project "Biometallics" (No. 08249103) to E.K. and a Grant-in-Aid for Scientific Research (C) (No. 10672089) to T.K.

Supporting Information Available: Tables of crystallographic parameters, atomic coordinates, equivalent isotropic temperature factors, anisotropic temperature factors, bond distances, bond angles, and torsion angles in CIF format as well as a complete X-ray structure report for **10**(ClO$_4$)$_2$. This material is available free of charge via the Internet at http://pubs.acs.org.

JA982904E

(34) Martell, A. E.; Motekaitis, R. J. *Determination and Use of Stability Constants*, 2nd ed.; VCH: New York, 1992.